

Phase and microstructural analysis of NdTi_{0.8}M_{0.2}O_{3.4} (M = Al, Ga) microwave ceramics

Raz Muhammad¹, Amir Khesro¹

¹ Department of Physics, Abdul Wali Khan University Mardan, Mardan, Khyber-Pakhtunkhwa, Pakistan.
e-mail: raz@awkum.edu.pk, amirkhesro@awkum.edu.pk

ABSTRACT

In this paper, we report the characterization of NdTi_{0.8}M_{0.2}O_{3.4} (M = Ga, Al) ceramics prepared *via* mixed oxide solid state sintering route. X-ray diffraction analysis of the samples revealed the formation of single phase for NdTi_{0.8}Ga_{0.2}O_{3.4} sample while secondary phase was formed in the case of NdTi_{0.8}Al_{0.2}O_{3.4}. Microstructural analysis of the sample showed dense packed grains. NdTi_{0.8}M_{0.2}O_{3.4} with M = Ga and Al exhibited a dielectric constant (ϵ_r) = 34, quality factor ($Q \times f$) = 9,776 and 10,867 GHz and temperature coefficient of resonance frequency (τ_f) = -113 and -90 ppm/°C, respectively. Further work is required on tuning the low τ_f of the samples for possible applications in the GHz frequency range.

Keywords: Ceramics; ABO_{3.4}, Perovskites, Microwave dielectric properties.

1. INTRODUCTION

The explosive development in the modern wireless communication industry such as cellular phones, base stations, wireless LAN, intelligent transport system (ITS) and microwave integrated circuits (MIC) has increased the demand for investigating new dielectric materials [1]. These applications require appropriate dielectric constant (ϵ_r), low dielectric loss or high quality factor ($Q \times f$), and near zero temperature coefficient of resonant frequency (τ_f) for devices such as resonators, filters, duplexers, and oscillators [2]. These parameters show the usage of material in different applications. Numerous compounds have been studied for their potential applications in the microwave region but still work is underway to explore new materials.

Dielectric materials show unique dielectric properties and are potential candidate materials for microwave devices. It is well known that among the three important characteristics (ϵ_r , $Q \times f$ and τ_f) of dielectric materials, dielectric losses are of prime importance. Dielectric losses depend on various factors including composition, processing and crystal structure [3, 4]. Non-centrosymmetric materials exhibit high dielectric losses due to lack of inversion symmetry while centrosymmetric materials exhibit low dielectric losses. Dielectric losses fall into two categories (intrinsic and extrinsic losses). Intrinsic losses depend on the crystal structure and the interaction of phonons with the electric field while extrinsic losses depends on defects, crystal imperfections, cations ordering, microcracks, porosity, inner stresses and oxygen vacancies etc. [5-7]. The major contributor towards dielectric losses is extrinsic. On the hand, K is almost directly proportional to τ_f (in the absence of any phase transition) and can be controlled by dopants either at A- or B-site of the lattice while τ_f depends on the tilting schemes [8].

A_nB_nO_{3n+2} ($n = 5$) type layered perovskite structure are attractive materials for the production of passive microwave components in wireless communication systems [9-12]. These compounds consist of five corner shared octahedral slabs connected with each other. The crystal structure and dielectric properties of layered perovskites has received great attention in the last few years [13]. For example, Zinc-substituted Ca_{0.2}La_{0.8}TiO_{3.4} possesses $\epsilon_r = 57.6$, $Q \times f = 17,100$ GHz, $\tau_f = -4.9$ ppm/°C [14]. LaMg_{0.2}Ti_{0.8}O_{3.4} has been reported to exhibit $\epsilon_r = 29$, $Q \times f = 13,000$ GHz, $\tau_f = -22$ ppm/°C [15]. Manan and Qazi [16] reported Sr_{0.2}La_{0.8}Ti_{0.986}Zr_{0.014}O_{3.4} which exhibited $\epsilon_r = 55$, $Q \times f = 11,960$ GHz and $\tau_f = 5.2$ ppm/°C. Similarly, NaCa₄Ta₅O₁₇ has been reported to exhibit $\epsilon_r = 41$, $Q \times f = 11,595$ GHz and $\tau_f = -14$ ppm/°C [17]. The microwave dielectric properties of NdTi_{0.8}M_{0.2}O_{3.4} (M = Al, Ga) phases have not been studied previously, therefore, in the present study, we have characterized NdTi_{0.8}M_{0.2}O_{3.4} (M = Al, Ga) ceramics and investigated their microwave dielectric properties.

2. MATERIALS AND METHODS

NdTi_{0.8}M_{0.2}O_{3.4} (M = Al, Ga) ceramics were prepared through solid state route using Nd₂O₃, TiO₂, Al₂O₃ and Ga₂O₃ as starting raw materials. In the first step, Nd₂O₃, TiO₂, and Al₂O₃ were dried at 800 °C for 6 h while Ga₂O₃ was dried at 500 °C for 6 h, to remove hydroxyl ions and moisture for accurate weighing of 20 g batches. The dried powders were weighted according to the molar ratios of the compositions and then mixed / milled in polyethylene jars, using yttrium stabilized zirconia balls as a grinding media and isopropanol as a liquid medium. The slurries were dried at 85 °C and then sieved through mesh (size 300 μm). The sieved powders were calcined in crucibles at 1250 °C for 6 h, at a heating / cooling rate of 5 °C/min. The calcined powders were re-milled to dissociate agglomerates (if any). The re-milled powders were pressed into pellets in a 10 mm steel die using a uniaxial pellet presser at 100 MPa. These pellets were sintered in the temperature range 1475-1650 °C for 4 h, at a heating / cooling rate of 5 °C/min.

Densities of the pellets were measured using an MD-300s electronic densitometer, based on Archimedes principle. Phase analysis of the samples was carried out using a D-5000 Siemens X-ray diffractometer (with Cu K α radiation). Raman spectra of the samples were collected using Renishaw microscope system (New Mills, Wotton-Under-Eagle, UK) with a diode 514 nm excitation laser. Microstructure of the samples was examined using FEI Inspect-F Scanning Electron Microscope with built-in EDS system. For microstructural analysis, samples were mechanically polished, thermally etched and coated with carbon. Microwave dielectric properties of the samples were measured using resonant cavity method [18]. τ_f was calculated in temperature range ~20 to 70°C using the formula

$$\tau_f = (f_2 - f_1) / (f_1 / (\Delta T))$$

where f_1 and f_2 are the resonance frequency at room temperature and 70°C.

3. RESULTS AND DISCUSSION

Figure 1 illustrates the room temperature XRD patterns of NdTi_{0.8}Ga_{0.2}O_{3.4} and NdTi_{0.8}Al_{0.2}O_{3.4} samples sintered at 1500 and 1600 °C for 4 h. The XRD pattern for NdTi_{0.8}Ga_{0.2}O_{3.4} (Fig. 1a) matched JCPDS#04-009-0684, for orthorhombic structure (Pnn2 symmetry). The refined lattice parameters were $a = 5.4522(17)$ Å, $b = 31.166(8)$ Å, $c = 3.8441(12)$ Å and $V = 653.2(3)$ Å³. The XRD pattern for NdTi_{0.8}Al_{0.2}O_{3.4} (Fig. 1b) matched JCPDS#04-009-0684; however, a secondary phase was also formed which matched JCPDS#04-017-8183 for CaLa₈Ti₉O₃₁ i.e. the major phase belongs to $n = 5$ and the secondary phase belongs to $n = 4.5$ series of A_nB_nO_{3n+2} type layered perovskite structure.

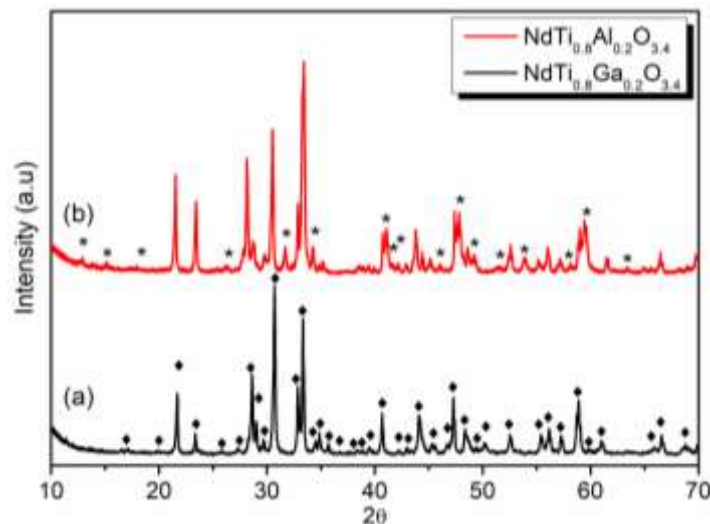


Figure. 1: XRD patterns of sintered a) NdTi_{0.8}Ga_{0.2}O_{3.4} and b) NdTi_{0.8}Al_{0.2}O_{3.4} ceramics, showing the formation of single phase for NdTi_{0.8}Ga_{0.2}O_{3.4} and a secondary phase for NdTi_{0.8}Al_{0.2}O_{3.4} ceramics.

The room temperature Raman spectra for NdTi_{0.8}Ga_{0.2}O_{3.4} and NdTi_{0.8}Al_{0.2}O_{3.4} samples are shown in Fig. 2. Within the studied range, a total of 11 active bands are observed for the sample LaTi_{0.8}Ga_{0.2}O_{3.4}. Amongst them the bands between 270-350 cm⁻¹ may be associated with B-site ordering and rotation of the

octahedral cage. The broad bands near 475-550 cm^{-1} may be due to symmetric breathing of BO_6 octahedra, while the strongest band near 768 cm^{-1} (referred to A_{1g} mode) along with a clear shoulder on lower frequency side can be ascribed to asymmetric breathing of the same octahedra. The band appearing near 603 cm^{-1} arises due to B-O stretching vibration. Based on the modes observed $\text{NdTi}_{0.8}\text{Ga}_{0.2}\text{O}_{3.4}$ is concluded to be isostructural to $\text{CaLa}_4\text{Ti}_5\text{O}_{17}$ [14], $\text{La}_5\text{Ti}_4\text{GaO}_{17}$ [19] and $\text{La}_5\text{Ti}_4\text{ScO}_{17}$ [20] which is also consistent with the present XRD result (Fig. 1a). However, for $\text{NdTi}_{0.8}\text{Al}_{0.2}\text{O}_{3.4}$ several additional modes appeared. The identification of these modes need further investigations but based on XRD results we suggest that extra modes may be due to the presence of secondary phases evident from XRD (Fig. 1b).

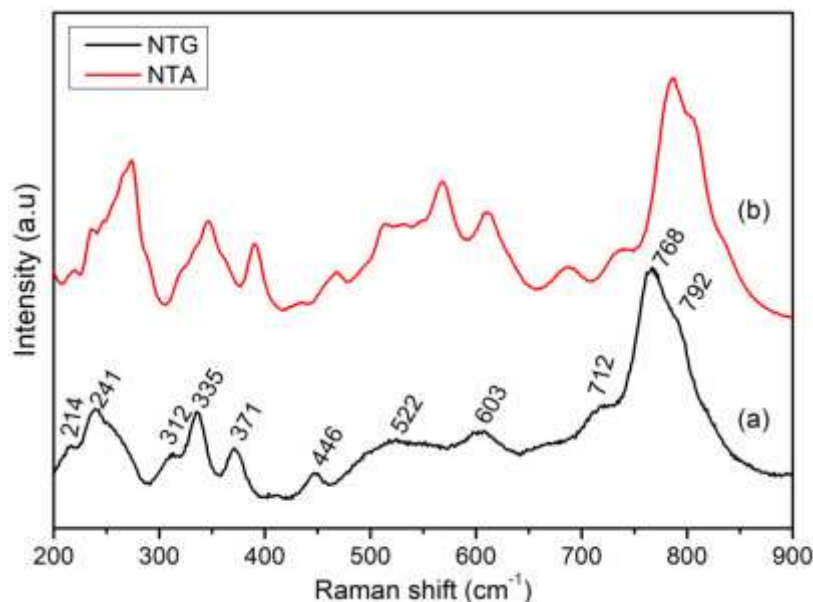


Figure 2: Room temperature Raman spectra of a) $\text{NdTi}_{0.8}\text{Ga}_{0.2}\text{O}_{3.4}$ and b) $\text{NdTi}_{0.8}\text{Al}_{0.2}\text{O}_{3.4}$ ceramics.

Plot of sintering temperature versus density is shown in Fig. 3. The density of the sample $\text{NdTi}_{0.8}\text{Ga}_{0.2}\text{O}_{3.4}$ increased with increasing sintering temperature from 1450 to 1500°C; however, no improvement in the density was observed upon further increase in temperature. Similarly, the optimum sintering temperature of the sample $\text{NdTi}_{0.8}\text{Al}_{0.2}\text{O}_{3.4}$ was found to be 1600°C. The SEM micrographs of the fractured surfaces of $\text{NdTi}_{0.8}\text{M}_{0.2}\text{O}_{3.4}$ (B = Ga, Al) ceramics sintered at their optimum sintering temperature are shown in Fig. 4. The sample $\text{NdTi}_{0.8}\text{Ga}_{0.2}\text{O}_{3.4}$ showed rod like grain morphology with size ranging from 1-9.3 μm . Fig. 4b illustrates the SEM micrograph for $\text{NdTi}_{0.8}\text{Al}_{0.2}\text{O}_{3.4}$ which shows two different types of grains (marked as A and B) which was further confirmed using EDS. The EDS spectra for both grain A and B are shown in Fig. 5. The grain 'A' shows smaller concentration of Al while grain 'B' shows higher concentration of Al. Therefore, the EDS results showed that grain 'A' and 'B' belongs to $\text{NdTi}_{0.8}\text{Al}_{0.2}\text{O}_{3.4}$ and $\text{Nd}_9\text{Ti}_8\text{AlO}_{31}$ phases, consistent with the XRD and Raman data.

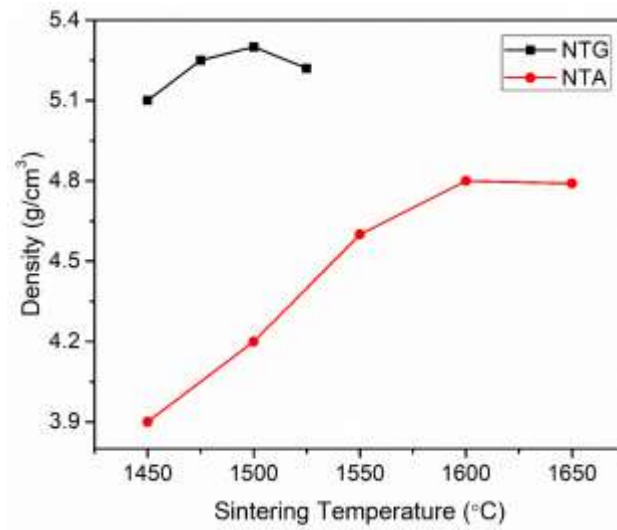


Figure 3: Plot of apparent density versus sintering temperature for $\text{NdTi}_{0.8}\text{M}_{0.2}\text{O}_{3.4}$ (B = Ga, Al) ceramics.

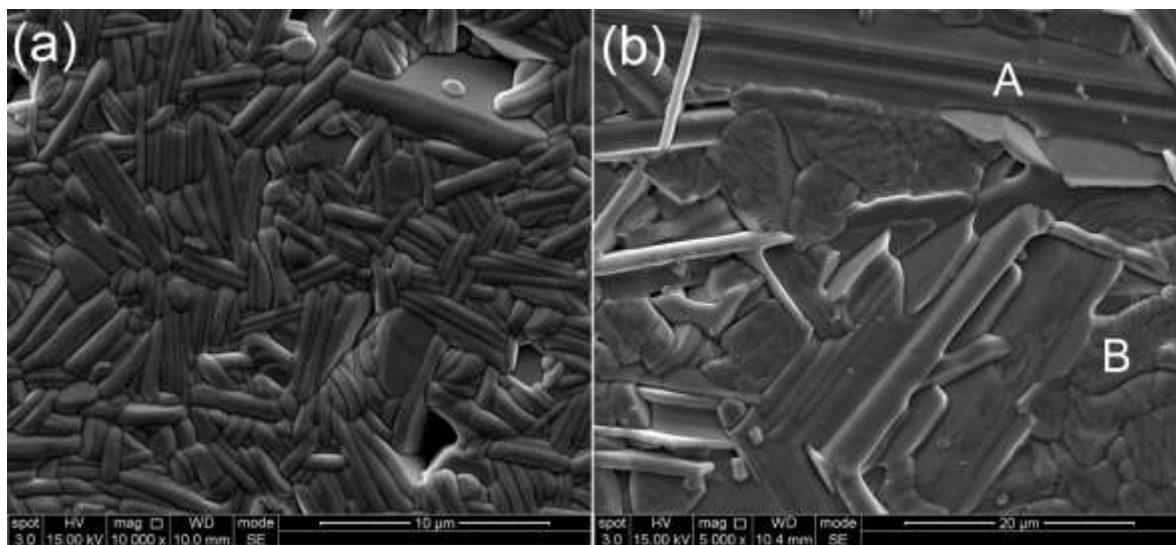


Figure 4: SEM images for a) $\text{NdTi}_{0.8}\text{Ga}_{0.2}\text{O}_{3.4}$ and b) $\text{NdTi}_{0.8}\text{Al}_{0.2}\text{O}_{3.4}$ ceramics sintered at 1500 and 1600°C for 4 h, respectively.

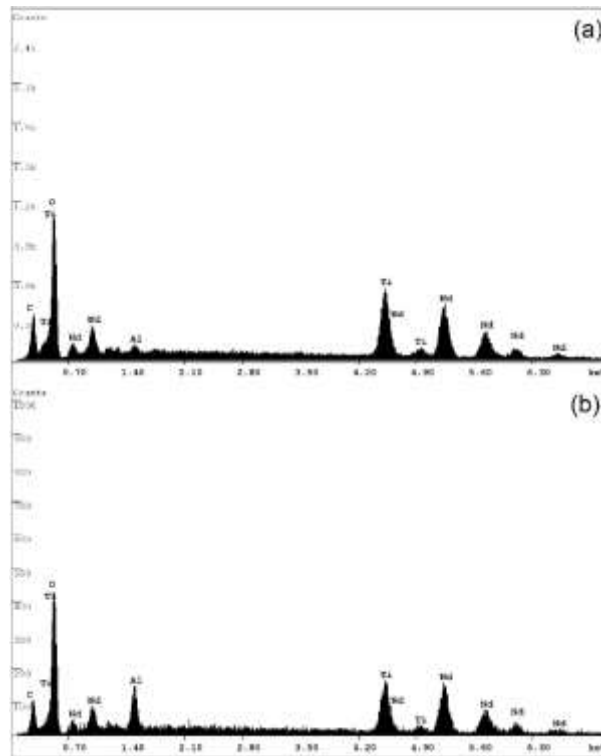


Figure 5: EDS spectra for the grain ‘A’ and ‘B’ for sample $\text{NdTi}_{0.8}\text{Al}_{0.2}\text{O}_{3.4}$, showing different concentration of Al in both grains

At optimum sintering temperatures, both $\text{NdTi}_{0.8}\text{Ga}_{0.2}\text{O}_{3.4}$ and $\text{NdTi}_{0.8}\text{Al}_{0.2}\text{O}_{3.4}$ samples exhibited similar values of K . Generally, it has been reported that low polarizable cation may decrease K and the $\text{NdTi}_{0.8}\text{Al}_{0.2}\text{O}_{3.4}$ sample should have lower K than $\text{NdTi}_{0.8}\text{Ga}_{0.2}\text{O}_{3.4}$ because of lower ionic polarizability of Al ($\alpha = 0.79 \text{ \AA}^3$) than Ga ($\alpha = 1.5 \text{ \AA}^3$) [21]. This statement may be true for single phase ceramics because the two different phases may have different contributions. However, $Q \times f$ of the sample $\text{NdTi}_{0.8}\text{Al}_{0.2}\text{O}_{3.4}$ was larger than $\text{NdTi}_{0.8}\text{Ga}_{0.2}\text{O}_{3.4}$ which may be possibly related to smaller ionic radii of the Al^{3+} (0.535 \AA) than Ga^{3+} (0.62 \AA) which decrease the an-harmonic lattice vibrations, resulting into low dielectric losses [22]. τ_f for $\text{NdTi}_{0.8}\text{Ga}_{0.2}\text{O}_{3.4}$ and $\text{NdTi}_{0.8}\text{Al}_{0.2}\text{O}_{3.4}$ samples were observed to be -113 and $-90 \text{ ppm/}^\circ\text{C}$. The τ_f values are quite low but to move it towards the ideal value of zero, further investigations needs to be done.

4. CONCLUSIONS

$\text{NdTi}_{0.8}\text{M}_{0.2}\text{O}_{3.4}$ ($B = \text{Ga}, \text{Al}$) samples were prepared via mixed oxide route and characterized using XRD, Raman, SEM, EDS and Vector Network Analyzer. The $\text{NdTi}_{0.8}\text{Ga}_{0.2}\text{O}_{3.4}$ sample was single phase while in the case of $\text{NdTi}_{0.8}\text{Al}_{0.2}\text{O}_{3.4}$, the two different phases were observed i.e. $\text{NdTi}_{0.8}\text{Al}_{0.2}\text{O}_{3.4}$ and $\text{Nd}_9\text{Ti}_8\text{AlO}_{31}$, which were further confirmed using Raman, SEM and EDS techniques. $\text{NdTi}_{0.8}\text{Ga}_{0.2}\text{O}_{3.4}$ exhibited a $K = 34$, $Q \times f = 9,776 \text{ GHz}$ and $\tau_f = -113 \text{ ppm/}^\circ\text{C}$, while sample $\text{NdTi}_{0.8}\text{Al}_{0.2}\text{O}_{3.4}$ exhibited 34 , $Q \times f = 10,867 \text{ GHz}$ and $\tau_f = -90 \text{ ppm/}^\circ\text{C}$. Further modification in the compositions is required for tuning the low τ_f through zero.

5. ACKNOWLEDGMENTS

The authors acknowledge the laboratory support provided by Functional Materials and Devices Group, Department of Materials Science and Engineering, University of Sheffield, UK.

6. BIBLIOGRAPHY

[1] SEBASTIAN, M., UBIC, R., JANTUNEN, H., “Low-loss dielectric ceramic materials and their properties”, *Int. Mater. Rev.*, v. 60, n. 7, pp. 392-412, 2015.

- [2] REANEY, I.M., IDDLES, D., “Microwave dielectric ceramics for resonators and filters in mobile phone networks”, *J. Am. Ceram. Soc.*; v. 89, pp. 2063-2072, 2006.
- [3] HU, L., ZHOU, H., SUN, Q., *et al.*, “Effects of ZrO₂-ZnO on the sintering behavior and microwave dielectric properties of 0.65CaTiO₃-0.35SmAlO₃ ceramics”, *J. Mater. Sci.: Mater. Electron.*; v. 27, pp. 12834-12839, 2016.
- [4] HUANG, J., ZHOU, H., WANG, N., *et al.*, “Preparation, structure and microwave dielectric properties of 3MgO-Al₂O₃-3TiO₂ ceramics”, *J. Mater. Sci.: Mater. Electron.*, v. 28, n. 6, pp. 4565-4569, 2016.
- [5] LI, L., LI, S., TIAN, T., *et al.*, “Microwave dielectric properties of (1-x)MgTiO₃-x(Ca_{0.6}Na_{0.2}Sm_{0.2})TiO₃ ceramic system”, *J. Mater. Sci.: Mater. Electron.*, v. 27, pp. 1286-1292, 2016.
- [6] ZHANG, H., WANG, X., CHENG, Q., *et al.*, “Preparation of Li₂MoO₄ using aqueous solution method and microwave dielectric properties after sintering”, *J. Mater. Sci.: Mater. Electron.*, v. 27, pp. 5422-5426, 2016.
- [7] W. LEI, W.Z. LU, X.H. WANG, *et al.*, “Phase Composition and Microwave Dielectric Properties of ZnAl₂O₄-Co₂TiO₄ Low- Permittivity Ceramics with High Quality Factor”, *J. Am. Ceram. Soc.*; v. 94, pp. 20-23, 2011.
- [8] REANEY, I.M., COLLA, E.L., SETTER, N., “Dielectric and structural characteristics of Ba-and Sr-based complex perovskites as a function of tolerance factor”, *Jap. J. Appl. Phys.*; v. 33, pp. 3984-3990, 1994.
- [9] JAWAHAR, I.N., SANTHA, N.I, SEBASTIAN, M.T, *et al.*, “Microwave Dielectric Properties of MO-La₂O₃-TiO₂ (M= Ca, Sr, Ba) Ceramics”, *J. Mater. Res.*; v. 17, pp. 3084-3089, 2002.
- [10] CHEN, Y.C., TSAI, J.M., “Influence of CuO addition and sintering temperature on microwave dielectric properties of Ca_{0.99}Zn_{0.01}La₄Ti₅O₁₇ ceramics for application in stacked patch antenna”, *Jap. J. Appl. Phys.*; v. 47, pp. 7959-7962, 2008.
- [11] DEMŠAR, K., ŠKAPIN, S.D., MEDEN, A., *et al.*, “Rietveld Refinement and Dielectric Properties of CaLa₄Ti₅O₁₇ and SrLa₄Ti₅O₁₇ Ceramics”, *Acta Chim. Sloven.*; v. 55, pp. 966-972, 2008.
- [12] MUHAMMAD, R., IQBAL, Y., “Preparation and characterization of K-substituted NaCa₄Nb₅O₁₇ microwave dielectric ceramics”, *J. Mater. Sci.: Mater. Electron.*; v. 24, pp. 2322-2326, 2013.
- [13] LI, C., WEI, X., FANG, L., “Dielectric and complex impedance analysis of Sr₅Nb₄TiO₁₇ ceramic with perovskite-like structure”, *J. Mater. Sci.: Mater. Electron.*; v. 26, pp. 8714-8719, 2015.
- [14] ZHAO, F., YUE, Z., GUI, Z., *et al.*, “Effects of zinc substitution on crystal structure and microwave dielectric properties of CaLa₄Ti₅O₁₇ ceramics”, *J. Am. Ceram. Soc.*; v. 89, pp. 3421-3425, 2006.
- [15] VANDERAH, T.A., MILLER, V., LEVIN, I., *et al.*, “Phase relations, crystal chemistry, and dielectric properties in sections of the La₂O₃-CaO-MgO-TiO₂ system”, *J. Solid State Chem.*; v. 177, pp. 2023-2038, 2004.
- [16] MANAN, A., QAZI, I., “Synthesis and microwave dielectric properties of Ca substituted SrLa₄Ti_{4.93}Zr_{0.07}O₁₇ ceramics”, *Bull. Mater. Sci.*; v. 37, pp. 679-683, 2014.
- [17] MUHAMMAD, R., IQBAL, Y., RAMBO, C.R., “Structure-property relationship in NaCa₄B₅O₁₇ (B = Nb, Ta) perovskites”, *J. Mater. Sci.: Mater. Electron.*; v. 26, pp. 2161-2166, 2015.
- [18] LONG, S., MCALLISTER, M., SHEN, L., “The resonant cylindrical dielectric cavity antenna”, *IEEE T. Antenn. Propag.*; v. 31, pp. 406-412, 1983.
- [19] MUHAMMAD, R., IQBAL, Y., REANEY, I.M., “Structure and microwave dielectric properties of La_{5-x}Sr_xTi_{4+x}Ga_{1-x}O₁₇ ceramics”, *J. Mater. Res.*; v. 50, pp. 3510-3516, 2015.
- [20] MUHAMMAD, R., KHESRO, A., NICHOLLS, S.J., “Layered perovskite structured La_{5-x}Sr_xTi_{4+x}Sc_{1-x}O₁₇ microwave ceramics for dielectrically loaded antennas”, *Ceram. Int.*; v. 42, pp. 6422-6427, 2015.
- [21] SHANNON, R.D., “Dielectric polarizabilities of ions in oxides and fluorides”, *J. Appl. Phys.*; v. 73, pp. 348-366, 1993.
- [22] SEBASTIAN, M., SANTHA, N., BIJUMON, P., *et al.*, “Microwave dielectric properties of (1-x)CeO₂-xCaTiO₃ and (1-x)CeO₂-xSm₂O₃ ceramics”, *J. Eur. Ceram. Soc.*; v. 24, pp. 2583-2589, 2004.

ORCID

Raz Muhammad <https://orcid.org/0000-0001-5482-7677>
Amir Khesro <https://orcid.org/0000-0002-0015-9332>